

A deep X-ray observation of M82

Piero Ranalli¹

¹ Università di Bologna, Dipartimento di Astronomia, via Ranzani 1, 40127 Bologna, Italy
E-mail: piero.ranalli@bo.astro.it

ABSTRACT

The main results from a deep X-ray observation of M82 are summarised: spatially-dependent chemical abundances, temperature structure of the gas, charge-exchange emission lines in the spectrum. We also present an update of the chemical abundances, based on a more refined extraction of spectra.

KEY WORDS: galaxies: individual: M82 – galaxies: abundances – X-rays: ISM

1. Main results

We performed a very deep (100 ks) observation of the starburst galaxy M82 with the EPIC and RGS instruments on-board the X-ray telescope XMM-*Newton*. The analysis has been published in Ranalli et al. (2008); we refer for any detail to that paper. A brief summary of the main results is presented in the following.

At least three spectral components are present in the broad-band spectrum: i) continuum emission from point sources; ii) thermal plasma emission from hot gas; iii) charge exchange emission from neutral metals (Mg and Si). The plasma emission has a double-peaked differential emission measure.

The chemical absolute abundances depend on the distance from the galactic plane, being larger in the outskirts and smaller close to the galaxy centre. The abundance ratios also show spatial variations. This might be due to the dependence of supernova (SN) yields on the progenitor mass, if the matter expelled by the first SN in a burst of star formation is also the first one to travel out of the galactic plane. It may also represent a clear example of metals being pushed in the inter-galactic medium.

The X-ray derived Oxygen abundance is lower than that measured in the atmospheres of red supergiant stars, leading to the hypothesis that a significant fraction of Oxygen ions has already cooled off and no longer emits at energies $> \sim 0.5$ keV.

2. Spatially-dependent chemical abundances

The gaseous outflow was divided in eleven slices, each one being parallel to the galactic plane, and spectra were extracted and analysed for each slice, deriving the temperature structure, abundances, and physical parameters of the plasma. We discovered that the regions used for spectral extractions in Ranalli et al. (2008) were actually larger than intended. However, no significant change in any conclusion or derived value has occurred. Nonethe-

less, here we publish the corrected figures and table.

The slices were numbered from N1 to N5, and from S1 to S5 with increasing height above the galactic plane; in the figures, negative heights are assigned to the northern regions. The spectral model was a multi-temperature APEC plasma, with components ranging from 0.1 to 10 keV. Point sources were excluded from all spectral regions except the galaxy centre, where their contribution was added to the model in the form of an absorbed power-law. The best-fitting abundances are shown in Fig. 1 (left panel) along with results from infrared observations for the central regions (Origlia et al. 2004) which show the abundances of stars born before the start of the current burst. Lighter α -elements are more concentrated in the outflow than in the centre. This effect is larger for elements with lower atomic mass, becomes less evident for Si and reverses for S. The centre/outskirt abundance ratio in the centre is about $\sim 1/10$ for O and Ne. Fe is also more concentrated in the outflow.

The abundances ratios (Fig. 1 right panel) have smaller variations, and present different trends for light and massive elements: while the O/Fe and Ne/Fe ratios are lower in the centre than in the outskirts, the opposite holds for Si/Fe and S/Fe, with Mg/Fe being an intermediate case showing no variation. The scatter between values for centre and outskirts is a factor $< \sim 3$.

The physical parameters of the plasma may be obtained from the best-fitting temperature and normalisation of the model, with some assumptions about the volume and filling factor. From Table 1, one may see that the gas density and pressure decrease by a factor of ~ 10 from the centre to the outskirts, while the cooling time increases.

References

- Ranalli P. et al. 2008 MNRAS 386, 1464
 Origlia L. et al. 2004 ApJ 606, 862

	N5	N4	N3	N2	N1	centre	S1	S2	S3	S4	S5
Normalisation (10^{-5})	0.079	0.24	0.50	0.41	0.85	27	1.7	0.92	0.20	0.099	0.047
Volume (kpc^3)	0.61	1.2	1.1	0.43	0.41	1.4	0.24	0.35	0.26	0.21	0.22
Density (10^{-3} cm^{-3})	$2.6f^{-\frac{1}{2}}$	3.3	4.8	7.1	10	32	20	12	6.4	5.1	3.3
Pressure ($10^{-12} \text{ dine cm}^{-2}$)	$2.8f^{-\frac{1}{2}}$	3.5	5.7	10	18	54	32	19	9.2	6.1	3.6
Mass ($10^5 M_{\odot}$)	$0.40f^{+\frac{1}{2}}$	0.99	1.3	0.76	1.1	11	1.1	1.0	0.42	0.26	0.19
Energy (10^{53} erg)	$0.75f^{+\frac{1}{2}}$	1.9	2.9	1.9	3.2	33	3.3	2.9	1.1	0.56	0.36
Energy density ($10^{-12} \text{ erg cm}^{-3}$)	$4.1f^{+\frac{1}{2}}$	5.3	8.6	15	27	81	48	28	14	9.2	5.4
Cooling time (Myr)	$600f^{+\frac{1}{2}}$	500	380	360	300	100	150	250	400	380	490

Table 1. Physical parameters of the plasma across the different regions of the outflow. The dependencies on the filling factor f have been explicated for simplicity only in the first column, but they apply to all columns.

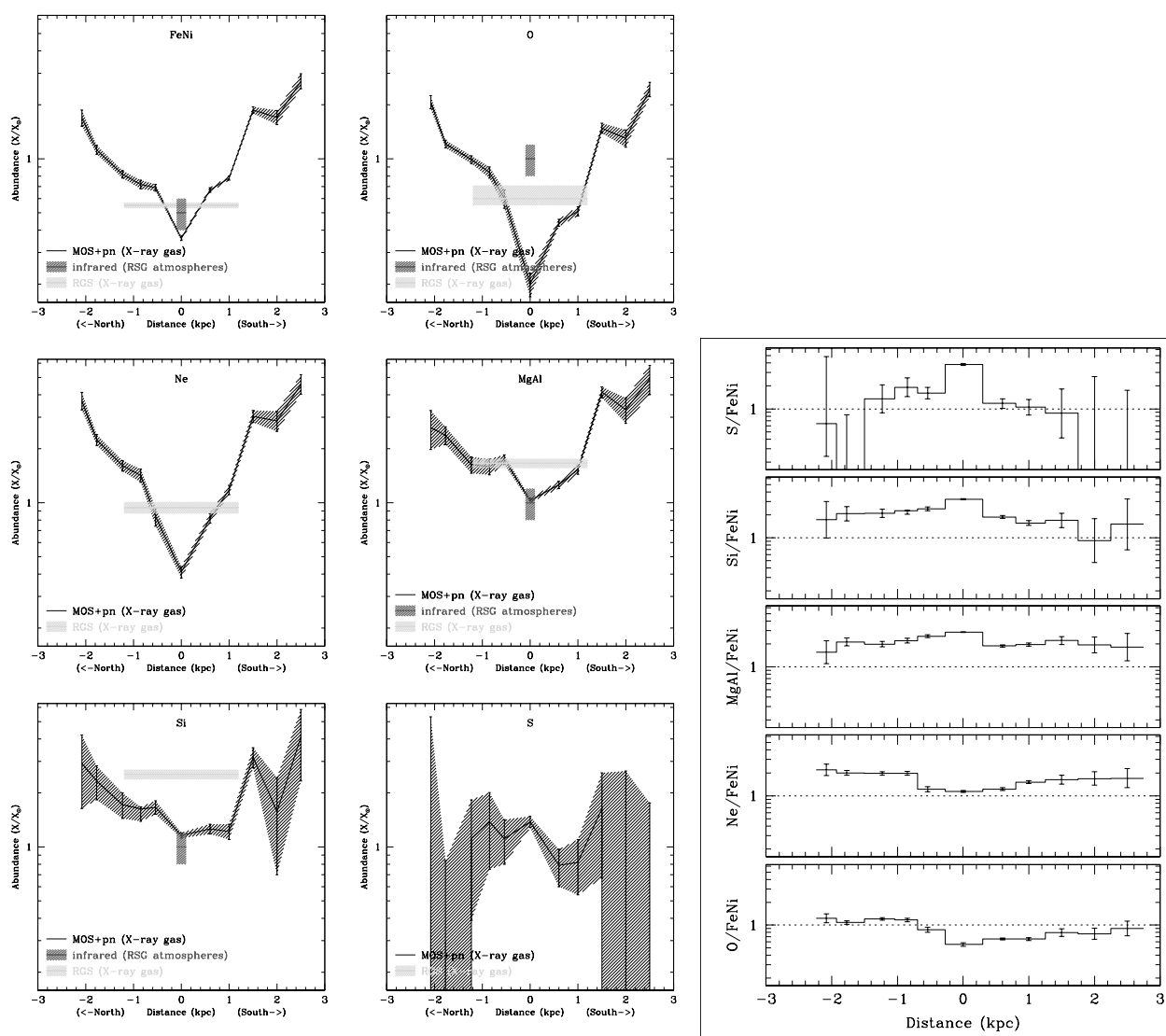


Fig. 1. *Left panels:* Variation of chemical abundances with increasing height on the galactic plane. Black: abundances from X-ray MOS and *pn* data. Blue: abundances from X-ray RGS data (due to the characteristics of the RGS spectrometer, they represent space-averaged values). Red: abundances from infrared data (corresponding to red supergiant stars in the galaxy central region). Negative values of distance refer to the north direction, positive values to south.

Right panel: Abundance ratios (X/Fe) observed in EPIC spectra of the outflow. Negative values of height refer to the north direction, positive values to south.